

**NANO EXPRESS**

**Open Access**

# Spontaneous formation of graphene-like stripes on high-index diamond C(331) surface

Maojie Xu<sup>1</sup>, Yaozhong Zhang<sup>1</sup>, Jing Zhang<sup>1</sup>, Jiyun Lu<sup>1</sup>, Bingjian Qian<sup>1</sup>, Dejong Lu<sup>1</sup>, Yafei Zhang<sup>1\*</sup>, Liang Wang<sup>2</sup>, Xiaoshuang Chen<sup>2</sup> and Hidemi Shigekawa<sup>3</sup>

## Abstract

We employ first-principles density functional theory calculations to study the surface reconstruction, energetic stability, and electronic structure of diamond C(331) surface. Spontaneous formation of graphene-like stripes on the reconstructed surface is found to occur as the surface terrace C atoms transform from  $sp^3$  to  $sp^2$  hybridization upon structural relaxation. The comparison of the calculated absolute surface energies of C(331), C(111), and C(110) surfaces demonstrates the energetic stability of the graphitic-like C(331) surface. Local density of electronic states analysis reveals the occurrence of localized electronic states near the Fermi level, which may have a significant impact on the surface conductivity.

**Keywords:** Surface reconstruction, Density functional theory, Graphene, Diamond

**PACS:** 68.35.bg, 68.47.Fg, 68.35.Md

## Background

Diamond holds a variety of extraordinary physical and chemical properties, facilitating its possible applications in novel functional devices [1-7]. As a semiconductor with a wide bandgap of 5.47 eV, it is a promising candidate for short-wavelength optoelectronic devices such as ultraviolet light-emitting diodes. The extreme mechanical hardness of diamond endows it with potential applications in nanomechanical devices. When doped with boron, it was found to display superconductivity around liquid helium temperature. To utilize the qualities of diamond, it is imperative to grow high-quality materials. Chemical vapor deposition is an efficient and versatile technique for the growth of diamond. A large body of experiments and theories are dedicated to understanding the growth process [8]. Graphitic-like surface reconstructions on stepped C(111) surfaces are predicated by first-principles calculations [9]. Surface graphitization of diamond nanoparticles is investigated from an experimental viewpoint [10]. A unique character of diamond growth is the existence of  $sp^2$ -hybridized bonds in the

graphitic-like layer of diamond surfaces, in contrast to other group IV element semiconductors (Si and Ge), which do not exhibit energetically favorable  $sp^2$  bonding configurations. This may account for different surface reconstructions on Si and diamond surfaces [11]. Besides low-index surfaces, high-index Si surfaces are extensively investigated to unveil their atomic and electronic structures [12,13], whereas less attention has been paid to the study of high-index diamond surfaces. The graphite-like  $sp^2$  bonding is expected to give rise to the significant difference between high-index diamond and Si surfaces.

Graphene, a two-dimensional atomic crystal with graphite-like  $sp^2$  bonding, has attracted considerable interests due to its novel physical and chemical properties and its potential applications in nanoelectronics and optoelectronics [14]. Large-scale graphenes are grown on metal substrates [15]. Here, we explore the formation of graphene-like stripes on a reconstructed high-index diamond C(331) surface using first-principles density functional theory (DFT) calculations. During the structural relaxation of the bulk-terminated surface, the terrace C atoms in the first layer delaminate from the second layer, leading to local  $sp^3$  to  $sp^2$  rehybridization and the formation of graphene-like stripes on the surface. The driving force for the graphitic-like

\* Correspondence: yfzhang@sjtu.edu.cn

<sup>1</sup>Key Laboratory for Thin Film and Microfabrication of the Ministry of Education, Research Institute of Micro/Nano Science and Technology, Shanghai Jiao Tong University, Shanghai 200240, People's Republic of China  
Full list of author information is available at the end of the article

reconstruction is the presence of high-density dangling bonds on the surface, which gives rise to the rebonding of top-layer atoms. The comparison of the calculated absolute surface energies of C(331), C(111), and C(110) demonstrates the relative stability of the C(331) surface with the graphitic-like reconstruction. Local density of electronic states (LDOS) analysis reveals the occurrence of localized electronic states near the Fermi level (FL), which may play an essential role in determining the surface conductivity [16,17].

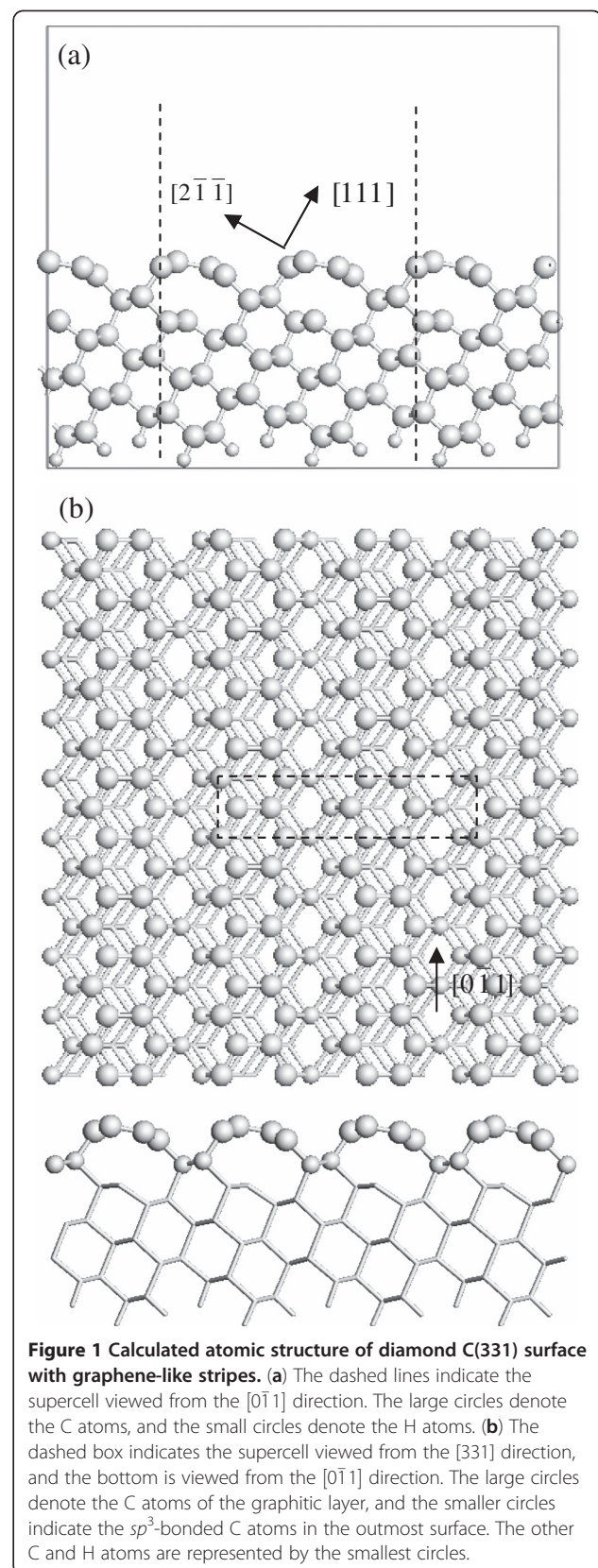
## Methods

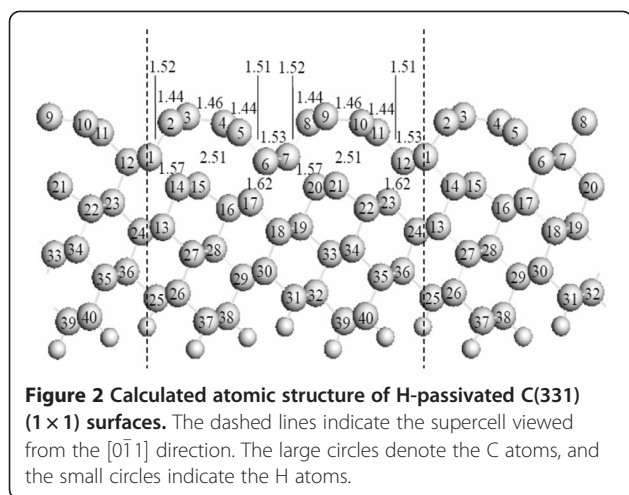
The calculations are conducted in the framework of the DFT method by DMol<sup>3</sup> codes [18]. We use the Perdew-Burke-Ernzerhof generalized gradient approximation [19]. A double numeric basis set including *d*-polarization function, all electron treatment, and an  $8 \times 2 \times 1$  Monkhorst-Pack *k*-point mesh for the Brillouin zone sampling [20] are employed to carry out geometry optimization and electronic band structure calculations. Spin-unpolarized self-consistent field calculations are performed with a convergence criterion of  $2.0 \times 10^{-5}$  hartree (1 hartree = 27.2114 eV) for total energies. The maximum force tolerance is 0.004 hartree  $\text{\AA}^{-1}$ , and the maximum displacement tolerance is 0.005  $\text{\AA}$ .

The periodically repeated slabs separated by approximately 10  $\text{\AA}$  of vacuum are used to represent the surface structures. Each slab of C(331) surface is composed of 11 atomic layers with 40 C atoms and 6 H atoms per unit cell. The H atoms are used to passivate the surface C atoms at the bottom of the slabs to make the calculation more efficient. The dashed lines in Figure 1a and the dashed box in Figure 1b indicate the supercell used for the calculation. Each slab of H-passivated C(331) surface is composed of 12 atomic layers with 40 C atoms and 12 H atoms per unit cell. The dashed lines in Figure 2 indicate the supercell used for the calculations.

## Results and discussion

Figure 1 shows the atomic structure of the graphene-like stripes formed on the reconstructed diamond C(331) surface calculated after the structural relaxation of the bulk-terminated surface. We allow this surface to relax using a steepest descent algorithm. The top-layer C atoms exhibit the  $sp^2$  bonding configuration in the graphene-like structure, as shown in Figure 1b. Upon structural relaxation, the terrace C atoms (see 4 and 10 C atoms in Figure 3) delaminate from the subsurface diamond and form the graphene-like stripes along the  $[0\bar{1}1]$  direction. The energetically favorable hexagonal rings are found to emerge in the graphitic layer on the reconstructed surface. The driving force for the graphitic-like reconstruction on the surface is the





presence of high-density dangling bonds which have unpaired electrons. This situation is similar to the reconstruction of the C(111) surface, where the top-layer C atoms are rearranged to make the dangling bonds become the nearest neighbors and form the  $\pi$  bonding [21]. For the C(331) surface, the delamination of the terrace C atoms can lead to the formation of graphite-like  $sp^2$  bonds, thereby reducing the energetically unfavorable dangling bonds.

The representative C-C bond lengths for the graphitic-like reconstructed C(331) surface are shown in Figure 3. The distance between the delaminated C atom and the subsurface C atom increases to approximately 2.51 Å, much larger than the bond length of diamond (1.54 Å). The bond lengths for the C atoms in the graphitic structure decrease to 1.44 and

1.46 Å. These values are quite close to the bond length of graphite (1.42 Å), whereas much smaller than that of diamond. The C atoms with the unsaturated dangling bonds at the subsurface positions remain  $sp^3$ -hybridized in character, although they have stretched by almost 34%. The C-C bonds are stretched to 1.62 and 1.57 Å for the outmost C atoms attached to the second-layer C atoms. The severe subsurface rebonding increases the elastic strain, which is energetically unfavorable. The competition between the favorable  $sp^2$  bonding in the graphitic layer and the unfavorable strain energy leads to the graphitic-like reconstruction of the C(331) surface.

The energetic stability of the C(331) surface is studied by comparing its absolute surface energy (ASE) with those of low-index diamond C(111) and C(110) surfaces [21-23]. In the centrosymmetric slab used for computing the ASE, the top and bottom surfaces are physically equivalent. After full structural relaxation, the same  $n \times m$  surface reconstruction is observed to occur on both sides of the slab. Therefore, it allows calculating directly the ASE. For the slab with  $N$  atoms at the atomic configuration  $\{R_i\}$ , the surface energy per  $1 \times 1$  surface cell,  $E_{\text{surf}}^{n \times m}$ , can be calculated from the total energy  $E_{\text{tot}}(N, \{R_i\})$  of the slab subtracted by  $N$  times the bulk diamond energy  $\mu$  per atom. The surface energy is expressed as

$$E_{\text{surf}}^{n \times m} = \frac{1}{2nm} \{E_{\text{tot}}(N, \{R_i\}) - N\mu\}. \quad (1)$$

Since two equivalent surfaces are involved in the calculations for a slab, a prefactor,  $\frac{1}{2}$ , is added in Equation 1.

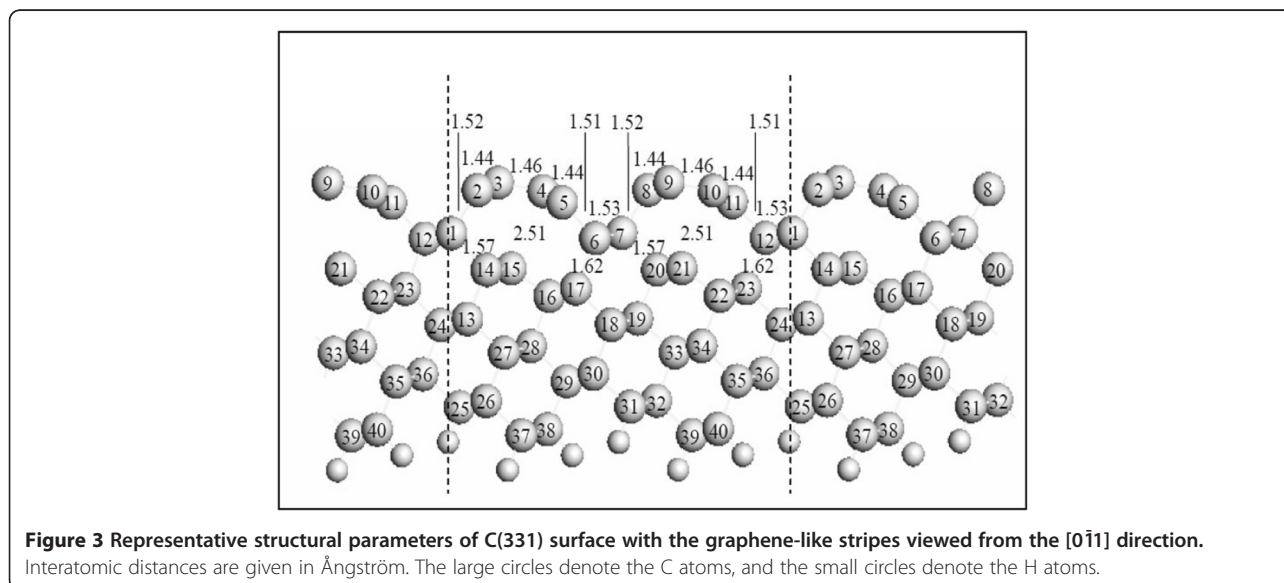


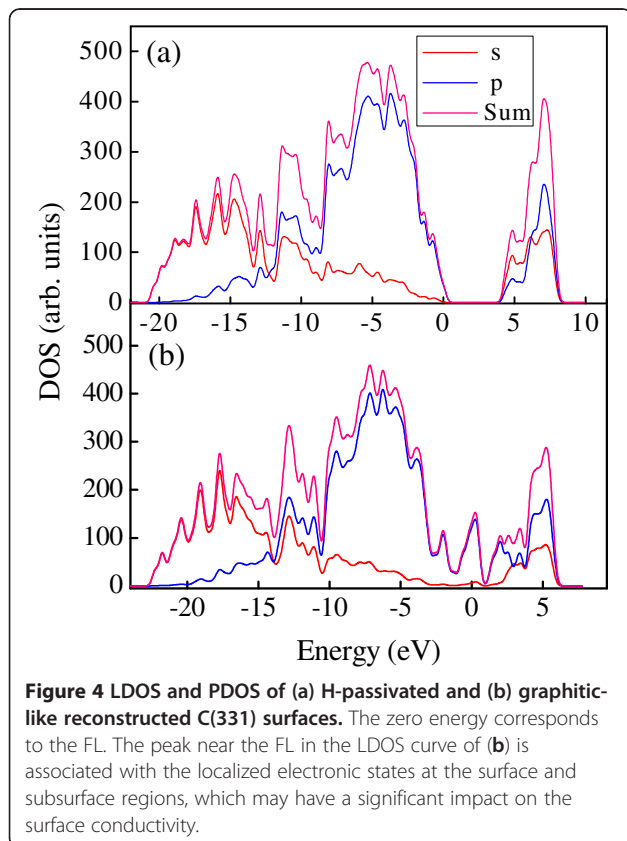
**Table 1 Absolute surface energies  $E_{\text{surf}}^{n \times m}$  and  $\gamma^{n \times m}$  for various orientations and reconstructions**

Orientation	Reconstruction	$E_{\text{surf}}$ (eV/1 × 1 cell)	$\gamma$ (J/m <sup>2</sup> )
(111)	2 × 1	0.993	2.91
		(1.369)	(4.06)
	H-covered	-1.903	-5.57
(110)	1 × 1 relaxed	1.824	3.27
		(3.264)	(5.93)
	H-covered	-4.971	-8.91
(331)	1 × 1 graphitic	2.040	2.31
		(-5.496)	(-9.99)
	H-covered	-5.808	-6.58

The values in parentheses from [21] are listed for comparison.

For the  $n \times m$  surface reconstruction, the  $nm$  gives the number of the  $1 \times 1$  surface cell. The surface energy per unit area is as follows:

$$\gamma^{n \times m} = \frac{E_{\text{surf}}^{n \times m}}{A}, \quad (2)$$



where  $A$  is the area of a  $1 \times 1$  surface cell for a given surface orientation  $n$ . For the H-covered C(331) surface, the surface energy per  $1 \times 1$  surface cell is given by

$$E_{\text{surf}}^{\text{H}} = \frac{1}{2} \{E_{\text{tot}}(N, N_{\text{H}}, \{R_i\}) - N\mu - N_{\text{H}}\mu_{\text{H}}\}, \quad (3)$$

where  $E_{\text{tot}}(N, N_{\text{H}}, \{R_i\})$  is the total energy of the slab,  $N_{\text{H}}$  is the number of H atoms, and  $\mu_{\text{H}}$  is the chemical potential of the H atom in the reservoir that is defined in [21]. Table 1 collected the surface energies  $E_{\text{surf}}^{n \times m}$ ,  $\gamma^{n \times m}$ , and  $E_{\text{surf}}^{\text{H}}$  for various orientations and reconstructions. The computed energies for low-index C(111) and C(110) surfaces agree well with the previous investigation [21]. The graphitic-like reconstructed C(331) surface is found to have lower  $\gamma^{n \times m}$  than low-index C(111) and C(110) surfaces, indicating that the C(331) surface is one of the stable crystalline diamond surfaces.

The H adsorption on the graphitic-like reconstructed C(331) surface is found to give rise to the reversion of  $sp^2$  hybridization back to  $sp^3$  hybridization. Figure 2 shows the calculated atomic structure of the H-covered C(331) ( $1 \times 1$ ) surface. The top-layer C atoms display  $sp^3$  bonding configuration. Thus, the H atoms can give rise to the dereconstruction of the graphitic-like C(331) surface.

Figure 4a shows the LDOS of the H-passivated diamond (331) surface. The zero energy corresponds to the FL which is at the position of the top valence band. An energy bandgap of 4.2 eV is obtained from the calculated electronic band structure. Figure 4b shows the LDOS of the reconstructed C(331) surface with the graphene-like stripes. The zero energy corresponds to the FL, which lifts up to a position in the bulk bandgap. The peak near the FL in the LDOS curve is attributed to the localized electronic states at the graphitic surface and subsurface regions, which may give rise to the semimetallic or metallic conduction along the surface. Further partial electronic density of states (PDOS) analysis reveals that the localized electronic states near the FL is predominant with the  $p$  character for the graphitic-like reconstructed C(331) surface.

## Conclusions

We carry out first-principles DFT calculations to study the spontaneous formation of graphene-like stripes on the reconstructed diamond C(331) surface. The  $sp^2$ -hybridized bonding in the graphitic layer on the surface plays a central role in reducing the energetically unfavorable dangling bonds on the bulk-terminated surface, thereby lowering the surface free energy. A sharp peak is found to occur near the FL in the LDOS curve, which arises from the localized electronic states at the surface and subsurface regions. These states may have a significant impact on the surface conductivity. The graphene-like stripes directly

formed on a semiconductor surface may be used for nanoelectronic and optoelectronic devices.

#### Abbreviations

ASE: absolute surface energy; DFT: density functional theory; FL: Fermi level; LDOS: local density of electronic states; PDOS: partial electronic density of states.

#### Competing interests

The authors declare that they have no competing interests.

#### Authors' contributions

MJX did the calculations and wrote the manuscript. YFZ conceived and suggested the calculations. YZZ, JZ, BJQ, JYL, DJL, LW, XSC, and HS discussed about the calculations and revised the final manuscript. All authors read and approved the final manuscript.

#### Authors' information

Dr. MJX obtained his Ph.D. from University of Tsukuba, Japan, and is currently working with Prof. YFZ as postdoctoral research fellow in Shanghai Jiao Tong University, China. Mr. YZZ, Ms. JZ, Mr. BJQ, Mr. JYL, and Mr. DJL are currently postgraduate students in Shanghai Jiao Tong University. Dr. YFZ obtained his Ph.D. from Lanzhou University, China, and is currently working as a professor in Shanghai Jiao Tong University. Dr. LW obtained his Ph.D. from Shanghai Institute of Technical Physics, Chinese Academy of Sciences, China, and is working with Prof. YFZ as postdoctoral research fellow. Dr. XSC obtained his Ph.D. from Nanjing University, China, and is currently working as a professor in Shanghai Institute of Technical Physics, Chinese Academy of Sciences, China. Dr. HS obtained his Ph.D. from Tokyo University, Japan, and is currently working as a professor in University of Tsukuba, Japan.

#### Acknowledgments

This work is supported by the National High-Tech R&D Program (863 Program) of China under contract no. 2011AA050504, the National Natural Science Foundation of China (grant no. 61006002), the U-M/SJTU Collaborative Research Program and the Analytical and Testing Center of SJTU.

#### Author details

<sup>1</sup>Key Laboratory for Thin Film and Microfabrication of the Ministry of Education, Research Institute of Micro/Nano Science and Technology, Shanghai Jiao Tong University, Shanghai 200240, People's Republic of China.

<sup>2</sup>National Laboratory for Infrared Physics, Shanghai Institute of Technical Physics, Chinese Academy of Sciences, Shanghai 200083, People's Republic of China. <sup>3</sup>Institute of Applied Physics, University of Tsukuba, Tsukuba 305-8573, Japan.

Received: 3 July 2012 Accepted: 30 July 2012

Published: 16 August 2012

#### References

1. Field JE: *The Properties of Natural and Synthetic Diamond*. New York: Academic; 1992.
2. Koide Y, Liao MY, Alvarez J, Imura M, Sueishi K, Yoshifusa F: **Schottky photodiode using submicron thick diamond epilayer for flame sensing**. *Nano-Micro Lett* 2009, **1**:30.
3. Isberg J, Hammersberg J, Johansson E, Wikstroem T, Twitchen DJ, Whitehead AJ, Coe SE, Scarsbrook GA: **High carrier mobility in single-crystal plasma-deposited diamond**. *Science* 2002, **297**:1670.
4. Purtov KV, Petunin AI, Burov AE, Puzyr AP, Bondar VS: **Nanodiamonds as carriers for address delivery of biologically active substances**. *Nanoscale Res Lett* 2010, **5**:631.
5. Liu YL, Sun KW: **Protein functionalized nanodiamond arrays**. *Nanoscale Res Lett* 2010, **5**:1045.
6. Jiang X, Zhao J, Zhuang C, Wen B, Jiang X: **Mechanical and electronic properties of ultrathin nanodiamonds under uniaxial compressions**. *Diam Relat Mater* 2010, **19**:21.
7. Jiang X, Zhao J, Jiang X: **Mechanical and electronic properties of diamond nanowires under tensile strain from first principles**. *Nanotechnology* 2011, **22**:405705.

8. Butler JE, Mankelevich YA, Cheesman A, Ma J, Ashfold MNR: **Understanding the chemical vapor deposition of diamond: recent progress**. *J Phys Condens Matter* 2009, **21**:364201.
9. Kern G, Hafner J: **Ab initio molecular-dynamics studies of the graphitization of flat and stepped diamond (111) surfaces**. *Phys Rev B* 1998, **58**:13167.
10. Chen J, Deng SZ, Chen J, Yu ZX, Xu NS: **Graphitization of nanodiamond powder annealed in argon ambient**. *Appl Phys Lett* 1999, **74**:3651.
11. Bechstedt F, Stekolnikov AA, Furthmüller J, Käckell P: **Origin of the different reconstructions of diamond, Si, and Ge (111) surfaces**. *Phys Rev Lett* 2001, **87**:16103.
12. Chadi DJ: **Theoretical study of the atomic structure of silicon (211), (311), and (331) surfaces**. *Phys Rev B* 1984, **29**:785.
13. Baski A, Erwin SC, Whitman LJ: **The structure of silicon surfaces from (001) to (111)**. *Surf Sci* 1997, **392**:69.
14. Castro Neto AH, Guinea F, Peres NMR, Novoselov KS, Geim AK: **The electronic properties of graphene**. *Rev Mod Phys* 2009, **81**:109.
15. Li XS, Cai WW, An JH, Kim S, Nah J, Yang DX, Piner R, Velamakanni A, Jung I, Tutuc E, Banerjee SK, Colombo L, Ruoff RS: **Large-area synthesis of high-quality and uniform graphene films on copper foils**. *Science* 2009, **324**:1312.
16. Balaban T, Klein DJ, Folden CA: **Diamond-graphite hybrids**. *Chem Phys Lett* 1994, **217**:266.
17. de Vita A, Galli G, Canning A, Car R: **Graphitization of diamond (111) studied by first principles molecular dynamics**. *Appl Surf Sci* 1996, **104**:297.
18. Delley B: **From molecules to solids with the DMol<sup>3</sup> approach**. *J Chem Phys* 2000, **113**:7756.
19. Perdew JP, Burke K, Ernzerhof M: **Generalized gradient approximation made simple**. *Phys Rev Lett* 1996, **77**:3865.
20. Monkhorst HJ, Pack JD: **Special points for Brillouin-zone integrations**. *Phys Rev B* 1976, **13**:5188.
21. Stekolnikov A, Furthmüller J, Bechstedt F: **Absolute surface energies of group-IV semiconductors: dependence on orientation and reconstruction**. *Phys Rev B* 2002, **65**:115318.
22. Marsili M, Pulci O, Bechstedt F, Del Sole R: **Electronic structure of the C (111) surface: solution by self-consistent many-body calculations**. *Phys Rev B* 2005, **72**:115415.
23. Silva F, Achard J, Bonnin X, Michau A, Tallaire A, Brinza O, Gicquel A: **3D crystal growth model for understanding the role of plasma pre-treatment on CVD diamond crystal shape**. *Phys Stat Sol (a)* 2006, **203**:3049.

doi:10.1186/1556-276X-7-460

**Cite this article as:** Xu et al.: Spontaneous formation of graphene-like stripes on high-index diamond C(331) surface. *Nanoscale Research Letters* 2012 **7**:460.

**Submit your manuscript to a SpringerOpen® journal and benefit from:**

- Convenient online submission
- Rigorous peer review
- Immediate publication on acceptance
- Open access: articles freely available online
- High visibility within the field
- Retaining the copyright to your article

Submit your next manuscript at ► [springeropen.com](http://springeropen.com)